2026 IEEE/SICE International Symposium on System Integration (SII)
January 11-14, 2026. Cancún, México

Proprioception-inspired Feedback for Robot Manipulation using Wearable Haptics

Tomoya Sasaki[1,2], Masahiko Inami[2], Domenico Prattichizzo[3,4]

Abstract— **Wearable haptic feedback has become an essential component in human-robot interaction, including teleoperation, prosthetics, and Supernumerary Robotic Limbs (SuperLimbs). However, most existing systems primarily convey contact or force information, and few address proprioception, the sense of body position and movement, which plays a key role in human motor control. In this paper, we propose a proprioception-inspired haptic feedback method using a wearable device that informs users of the movement state of a robot's end-effector. We implement two feedback strategies: Movement Haptic Feedback (MHF) and Error Haptic Feedback (EHF). Two user studies were conducted under disturbed visual conditions: one in a teleoperation scenario and another using a SuperLimb scenario. Results showed that both haptic feedback approaches improved task performance and reduced subjective workload compared to no-feedback conditions. These findings demonstrate the value of proprioception-inspired haptic design in expanding body awareness in human–robot sensory augmentation.**

I. Introduction

Wearable haptic feedback has been widely studied in robotics to improve operability in the areas of robotic prostheses [1]–[3], teleoperation [4], [5], cooperative robots [6], and wearable robots [7], [8]. Haptic feedback contributes to providing operators with rich information that complements audio and visuals. For example, the haptic representation of contact force supports object manipulation tasks using robots because the contact force of the robot with external environments and target objects cannot be ascertained by vision alone.

From the perspective of human body operation, we can see that the haptic sense is used not only when we are in contact with the environment or objects, but also in various other situations. For example, we have proprioception (or kinesthesia) [9], which is known as a part of the haptic sense, to recognize the self-position of the body. Proprioception is perceived not only by muscle contraction but also by skin deformation. A lack of proprioception is known to impair motor control. Previous work [10] has reported that patients with impairments of this sensory input have difficulty reaching targets accurately. In particular, errors in reaching tasks were significantly increased when visual information was restricted. In contrast, conventional robot manipulation rarely incorporates feedback designed for proprioception, resulting in a situation where operators rely almost entirely on visual information to infer the robot's state. Despite its importance, haptic feedback for conveying positional state has been little explored under conditions without visual information.

These limitations in positional awareness become more pronounced in teleoperation and SuperLimbs use, where visual information may be unreliable or temporarily unavailable and users cannot directly perceive the robot's posture through proprioception. These scenarios require simple and reliable cues that convey positional changes of the robot, especially during reaching tasks or sub-tasking in real-world environments.

In this study, we investigate how haptic feedback improves robot manipulation performance under disturbed visual information. To this end, using wearable haptics, we design stimuli inspired by proprioception that humans utilize to recognize their limb postures. We conduct two experiments under disturbed visual conditions in teleoperation and SuperLimbs scenarios. Both experiments were approved by the research ethics committee of The University of Tokyo (Approval No. 20-319). By comparing task performance using simple tasks, we discuss the potential and limitations of proprioception-inspired feedback. This study contributes to the design of sensory augmentation using wearable haptics for human-robot interaction (HRI) and human-computer interaction (HCI). In particular, we provide insights into proprioceptive stimulation for the design of human-robot sensory augmentation.

II. Related Work

A. Wearable Haptic Devices

Wearable haptics is one approach to providing haptic feedback using display technology [11], [12]. As the name suggests, wearable haptics involves devices worn on the body, and it has been explored to be worn on various parts of the body, such as fingertips, hands, arms, legs, and hips [13]. Various mechanisms have been proposed to provide haptic feedback in wearable haptics. For example, skin stretch, squeeze, and vibration have been proposed [14]. Skin stretch is a method of stretching and contracting the skin by placing contactors in close contact with the skin. For example, a mechanism using belts [15], [16], rollers [3], [17], and rotors [1], [18] has been proposed. Squeeze is a method of applying pressure to the entire area of target body parts. For example, bracelets [4], [19] and wristbands [20] have been proposed to be attached to the arm. Vibration is a method that uses eccentric rotating mass motors or linear actuators on the contact surface [21]. Further, methods combining these multiple mechanisms have also been proposed [19], [22].

[1]Faculty of Advanced Engineering, Tokyo University of Science, Japan
[2]RCAST, The University of Tokyo, Japan
[3]DIISM, University of Siena, Italy
[4]HHCM, Istituto Italiano di Tecnologia, Italy

978-1-6654-5784-2/26/$31.00 ©2026 IEEE

B. Proprioceptive Feedback

Proprioception is related to skin senses from the perspective of the physiological mechanism. Haptics sometimes handles proprioception using skin stretch approaches, known as proprioceptive feedback. Proprioceptive feedback is used in situations where humans operate robots, in particular, as robotic prostheses. For example, Bark et al. [18] and Wheeler et al. [1] studied a rotational skin stretch device that revealed the basic characteristics of the relationship between perceived haptic sensation and the amount of rotation of a rotor attached to the skin, and that proposed a system for application to the proprioceptive feedback of a myoelectric prosthetic hand. Rossi et al.'s HapPro [2] proposed a haptic device using a linearly moving contactor, and Colella et al.'s Stretch-Pro [3] proposed a haptic device with a roller mechanism contactor.

C. Wearable Haptics in Robot Manipulation

In HRI, wearable haptics is expected to improve usability and operability. Various applications have been studied in the past, such as teleoperation [4], [5] and Physical HRI (pHRI) [23], including handover tasks [24]. Recently, applications of wearable haptics in SuperLimbs [25]–[27] have been actively attempted [8], [28]–[30]. For example, Sasaki et al. [8], [28] implemented a haptic feedback mechanism in a controller for manipulating robot arms using the user's foot that provides information when the arm touches an object to the user. Guggenheim et al. [29] proposed haptic feedback via torque generation while the robotic limbs were in contact with the environment. Iwasaki et al.'s Detachable Body [30] showed a presenting method of the position of the end-effector of a robot arm using vibrotactile feedback that indicated the direction from the user's perspective.

III. Experimental Method

A. Stimuli Design

We design haptic stimuli that change in intensity according to the movement of the end-effector and adopt two feedback models: Movement Haptic Feedback (MHF), which reflects movement from the start point, and Error Haptic Feedback (EHF), which reflects positional error to the target. Although human proprioception integrates multiple sensory signals generated during body movement, directly reproducing such complex mechanisms in robot-manipulation scenarios may reduce usability. For example, presenting multi-channel stimuli derived from all joint-angle changes would impose high cognitive load, require long learning time, and complicate device implementation.

Because this study focuses on evaluating operability rather than developing sophisticated feedback mechanisms, we adopt a simple position-based approach. Positional information provides stable and intuitive cues for users during reaching, whereas velocity- or acceleration-based cues generally impose higher cognitive demands and are more difficult to interpret accurately. Therefore, MHF and EHF were selected as practical and accessible feedback models from both cognitive and implementation perspectives.

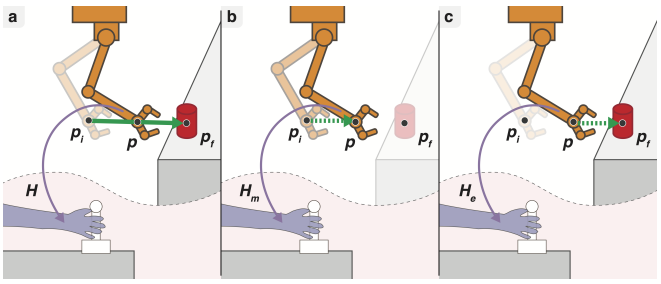

Fig. 1. (a) Coordinate setting for haptic stimulation, (b) Movement Haptic Feedback (MHF), (c) Error Haptic Feedback (EHF).

Based on this design choice, we formulate the problem as follows. We assume the user manipulates the end-effector of the robot arm using an input device as shown in Figure 1a. The end-effector moves from a starting point $\mathbf{p}_i$ to a target object $\mathbf{p}_f$. When the current position is $\mathbf{p}$, MHF presents stimulus proportional to the movement from $\mathbf{p}_i$ to $\mathbf{p}$ (Figure 1b), while EHF presents stimuli based on positional error from $\mathbf{p}$ to $\mathbf{p}_f$ (Figure 1c). We formulate the relationships between these quantities and the haptic intensities as:

$$H_m(\mathbf{p}) = \begin{cases} a \cdot \|\mathbf{p} - \mathbf{p}_i\|, & \text{if } \|\mathbf{p} - \mathbf{p}_i\| \leq \|\mathbf{p}_f - \mathbf{p}_i\| \\ b, & \text{otherwise} \end{cases} \quad (1)$$

$$H_e(\mathbf{p}) = b - a \cdot \|\mathbf{p}_f - \mathbf{p}\| \quad (2)$$

Where H_m and H_e are the haptic intensity presented to the user, respectively, a and b are constants for correction, and $\mathbf{p}$, $\mathbf{p}_i$, and $\mathbf{p}_f$ are the coordinates corresponding to Figure 1. The specification of the haptic presentation mechanism assumes the maximum value of the intensity it can present, and it is not possible to present negative intensity. In the MHF, the intensity is saturated at the maximum value when $\|\mathbf{p} - \mathbf{p}_i\|$ exceeds $\|\mathbf{p}_f - \mathbf{p}_i\|$, and in the EHF, the intensity increases again after passing the target.

These allow the control of haptic intensity based on the setting of the start, end, and current position of the end-effector. Although the above formulations are written in a general vector form, the experiments in this study involve one-dimensional reaching. Therefore, we consider a one-channel wearable haptic device and treat the norms as scalar distances in the following.

B. Wearable Haptic Device

1) Mechanism: The squeeze mechanisms for skin deformation are suitable for providing proprioceptive feedback, so we adopt a belt-based squeeze similar to the previous study [4] as the feedback mechanism of our prototype. Figure 2a shows the components of the feedback mechanism.

The squeezing mechanism consists of rotating actuators (motors) and a belt, which is wrapped around a limb to give feedback. As shown in Figure 2b, by rotating the two motors in opposite directions, the belt squeezes the wrapped area. The haptic intensity H_i presented by the device shall be

$$H_i = f_d(\theta_r) \quad (3)$$

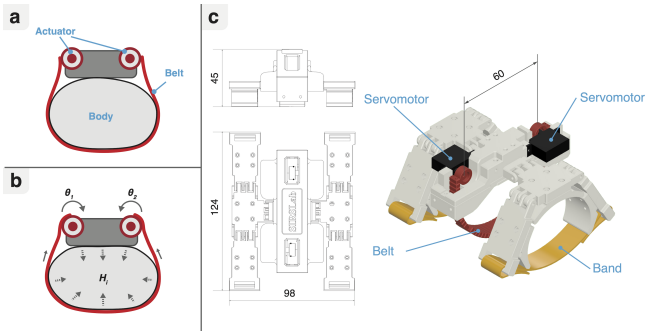

Fig. 2. (a) Components of the squeeze mechanism using a belt, (b) relationship between haptic intensity and motor angles, (c) design of the wearable device using a squeeze mechanism with a belt unit and band parts.

where θ_r is the haptic control rate, the motor's range of motion expressed as a percentage and is calculated by $\theta_i/(\theta_{max} - \theta_{min}) \times 100$. Note that the function f_d is affected by various factors such as the structure of a device, characteristics of actuators, and the condition of tactors, and it should be determined by using an implemented device.

2) Implementation: The configuration of the wearable device is shown in Figure 2c. The device consists of an actuator part for the belt mechanism and band parts for attaching to the user's body. The device has a belt mechanism unit to give haptic feedback with one degree of freedom. The external dimensions of the device are $124\times45\times98\mathrm{mm}$ in width, height, and depth before attaching, and its weight is $100\,\mathrm{g}$. Two HITEC HS-5035HD servo motors are used to squeeze, and the width between the motor shafts is $60\,\mathrm{mm}$. The angle range of the servomotors is 180 degrees. The device components and belt except electronics were made using a 3D printer. When the device is working, an exterior part covers the motors to conceal motor motion from the outside. The contact width of the belt to squeeze is $12\,\mathrm{mm}$ and the belt was made with a fixed length ($180\,\mathrm{mm}$). We ensure a certain level of contact by adjusting the attachment position with the band, although there is a difference in the user's physique. The servomotor is controlled from a PC via a microcontroller, Arduino Uno, with serial communication with the PC. We use Unity on the PC to control the device.

C. Parameter Determination

We determine the parameters of the wearable device implemented to conduct experiments. From Equation 3, haptic intensity is controlled by the change in the haptic control rate. In this study, we indirectly measure haptic intensity as a psychophysical quantity as a subjectively perceived intensity by humans, rather than a physical quantity of force generated by the belt mechanism. This allows us to obtain the relationship between the haptic control rate of the device and the amount of haptic feedback through the perceived intensity. From the obtained values, we determine the coefficients corresponding to Equations 1 and 2.

We conducted a psychophysical experiment using the magnitude estimation method, and the participants in the experiment were eight healthy males (aged between 23 and 30, with an average age of 25.1). From the results, we determined that a, b in Equations 1 and 2 were set to 1.957 and 2.971, respectively. Note that, during experiments, we also use other coefficients to normalize the movement and error quantities in each equation.

IV. Experiment 1: Teleoperation

We investigate the effects of haptic feedback on teleoperation while visual information is temporarily lost.

A. Setup and Apparatus

Figure 3a presents the experimental setup. Participants sit on a chair and grasp a lever-type input device with their right hand. They look at the display on the monitor during the experiment. The haptic device is attached to the right arm. The left hand operates the keyboard according to the experimental instructions. A headphone playing white noise is worn during the task. The lever-type input device is a self-made force plate, a lever attached to the top of the force plate, which consists of four pressure sensors (Interlink Electronics FSR 402) and an Arduino Pro Micro for serial communication with a PC. Participants can input force by tilting the lever back and forth while pushing it vertically. The input device is fixed to the desk. The PC we use in the experiment is a Razer Blade 15 with Intel Core i7-8750H processor and NVIDIA GeForce RTX 2070 running Windows 10. The monitor is an LG 24UD58-B 23.8-inch monitor (resolution: 3840×2160).

B. Task

We use a simple reaching task involving visual interferences where an end-effector moves along a vertical one-dimensional axis. Figure 3b shows the simulator screen with a red target and a cursor representing the end-effector of a robotic limb. The yellow scale represents units in the simulator (not on the actual screen), with a unit distance of $8\,\mathrm{mm}$ measured on the monitor. The simulator was developed using Unity. Participants use a lever-type input device to move the cursor toward the target. Inputs are made by tilting the lever while pressing it vertically (input range: $0.2\,\mathrm{N}$–$20\,\mathrm{N}$). The cursor position was updated by applying a constant to the pressure sensor value of the input device and adding it (0.00–10.00) every simulator cycle (average $20\,\mathrm{ms}$).

The task sequence, as shown in Figure 3c, includes three steps: 1) Displaying the initial positions of the cursor and target. 2) Following a 3-second countdown, participants get ready and then move the cursor to reach the target under Visual/Blind conditions. 3) Participants press a keyboard key with their left hand upon judging the cursor's arrival at the target. After completing one trial, the screen goes dark for a few seconds before the next trial begins. This sequence repeats for a set number of trials. The target's initial positions are randomly selected from four distances (6, 7, 8, and 9 units distance from the end-effector in Figure 3b). During the task, participants aim to align the cursor's concave part with the target swiftly and accurately. Screen displays in step 2 vary with different visual conditions described in Section IV-C.

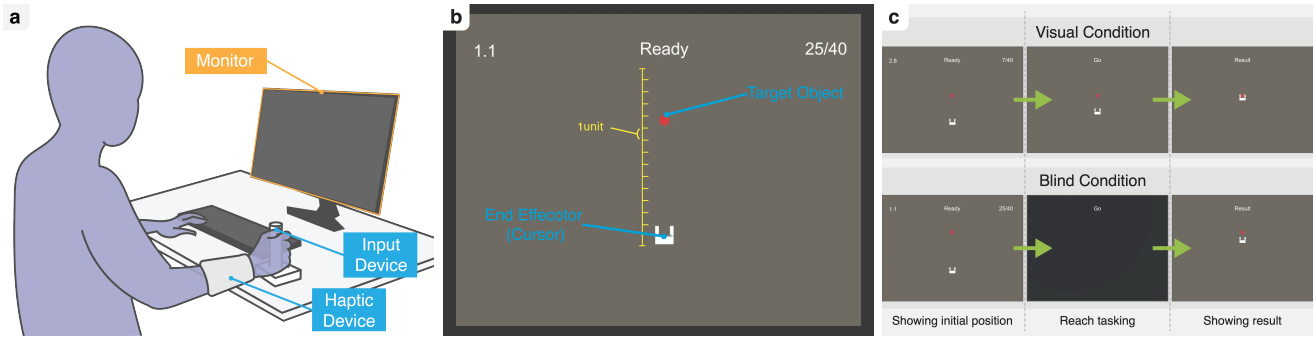

Fig. 3. (a) in the setup, participants use an input device and wear a haptic device, (b) the monitor shows a target and a cursor, (c) the task sequence and displayed information differ by visual condition.

C. Procedure and Participants

The reaching task is conducted under six conditions: a combination of two visual conditions (Visual and Blind) and three haptic conditions (NO, MHF, EHF). Visual condition differences relate to step 2 of the reaching task as described in Section IV-B, wherein in the Visual condition (Figure 3c top row), participants can see the cursor's movement during the reach. Conversely, in the Blind condition (Figure 3c bottom row), the screen hides all images seconds after showing the initial positions at the task's start, blocking cursor visibility during reaching. Participants must manipulate the cursor without visual information and press a keyboard once they judge it has reached the target. Afterward, the final positions are immediately revealed.

The experiment is divided into three sessions based on haptic feedback conditions: NO (no haptic feedback), and MHF and EHF (feedback by our design). Session 1 presents NO condition, while Sessions 2 and 3 present MHF or EHF, counterbalanced across participants. Each session includes practice (5 trials), visual condition trials (20 trials), and blind condition trials (20 trials), sequentially. After each trial, participants respond to the questionnaire created with reference to NASA-TLX [31] in Japanese, assessing subjective workload across six items: mental demand (MD: low/high), physical demand (PD: low/high), temporal demand (TD: low/high), performance (OP: good/bad), effort (EF: low/high), and frustration (FR: low/high). Finally, participants orally provide comments or feedback on the task.

The participants were 12 healthy adults (aged between 23 and 40 with an average age of 27.0, 10 males and 2 females). Two are left-handed.

D. Results

1) Completion Time: Figure 4 shows the results of the task completion time. The three bars on the left side are the scores for each haptic condition in the visual condition and the three on the right side are the scores for each haptic condition in the blind condition, respectively. The mean completion time for all conditions was 3.6 s (SD: $\pm$1.3 s). In the visual condition, the mean completion time was 3.4, 3.7, and 3.5s, respectively, from left to right (NO, MHF, and EHF), and 3.6, 3.5, and 3.8s, respectively in the blind condition. There was no tendency for the completion time to differ depending on the visual condition. We conducted a statistical analysis to confirm the differences due to the different haptic conditions. Since the Shapiro-Wilk test rejected normality, we conducted the Friedman test, confirming that there was a significant difference in the blind condition ($\chi^2(2) = 6.008$, $p = 0.050$). As a post hoc test, multiple comparisons were conducted using the Wilcoxon rank sum test using Bonferroni correction, and a significant difference was confirmed between MHF–EHF (adj. $p = 0.005$).

2) Accuracy: Figure 5 presents the task accuracy, and the vertical axis indicates the distance in the simulator. The mean distance error was -0.08, -0.09, and -0.06, respectively in the visual condition, from left to right (NO, MHF, and EHF), and 0.59, -0.08, and -0.03, respectively in the blind condition.

In the visual condition, there was no difference in the distance depending on the tactile presentation condition. In the blind condition, because there was a tendency depending on the haptic condition, we performed a statistical analysis. Since normality was rejected by the Shapiro-Wilk test, we conducted the Friedman test, confirming that there was the possibility of a significant difference in the blind condition ($\chi^2(2) = 6.008$, $p = 0.050$). As a post hoc test, multiple comparisons were conducted using the Wilcoxon rank sum test using Bonferroni correction, and significant differences were confirmed between NO–MHF (adj. $p = 0.011$) and NO–EHF (adj. $p = 0.023$). The distance error was significantly smaller for both MHF and EHF conditions than for NO condition. On the other hand, there was no difference between MHF and EHF (adj. $p = 1.000$).

3) Subjective Workload: Figure 6 shows the response scores of the subjective workload. The scores are converted from a 7-point Likert scale to percentages. As a general trend, we can confirm that the scores in the blind condition tend to be higher than those in the visual condition. Higher scores indicate a higher workload. This suggests that the task in the blind condition is more demanding than that in the visual condition. We conducted a statistical analysis to confirm the differences in the haptic conditions. Since normality was rejected by the Shapiro-Wilk test, we conducted the Friedman test. The results confirmed that there was the possibility of a significant difference in PD ($\chi^2(2) = 6.067$, $p = 0.048$) in the visual condition, MD ($\chi^2(2) = 12.409$, $p = 0.002$), OP ($\chi^2(2) = 9.3488$, $p = 0.009$), and FR ($\chi^2(2) =$

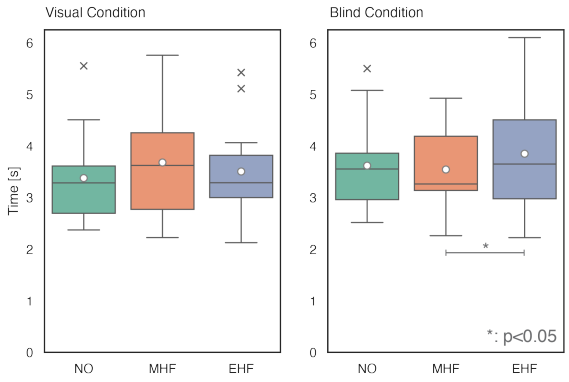

Fig. 4. Completion time

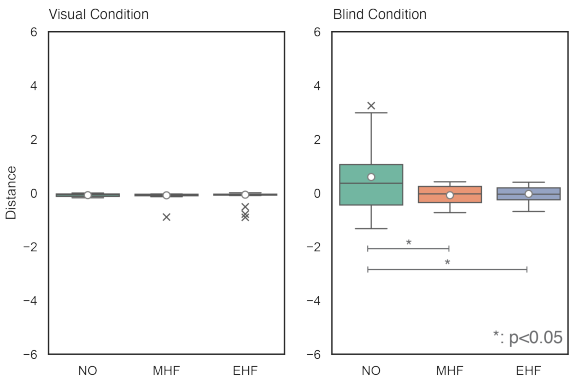

Fig. 5. Task accuracy

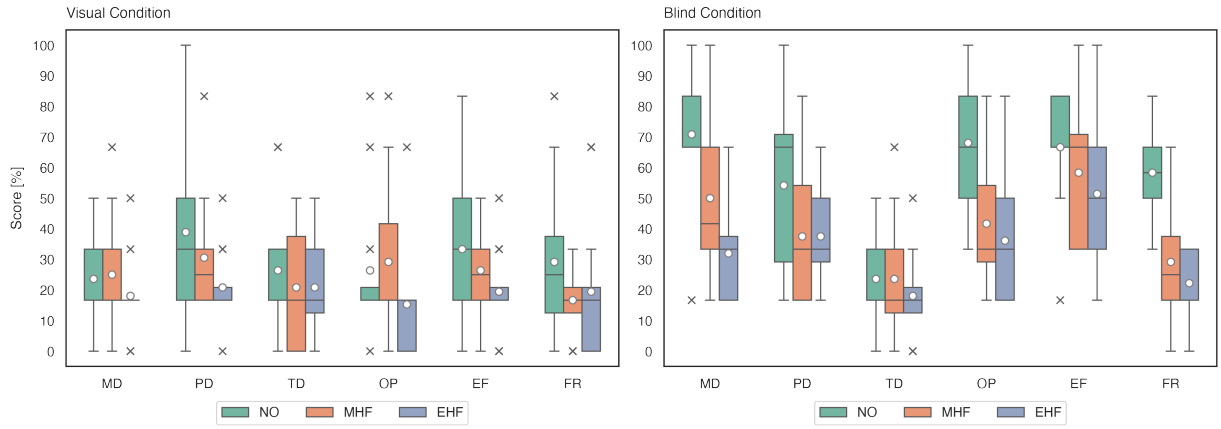

Fig. 6. Subjective task load

15.2, p = 0.001) in the blind condition. As post hoc tests, multiple comparisons were conducted using the Wilcoxon rank sum test using Bonferroni correction, and the results showed that there was a significant difference between NO–EHF for item MD (adj. p = 0.010), NO-EHF for item OP (adj. p = 0.036), and NO–MHF (adj. p = 0.018) and NO–EHF (adj. p = 0.010) for the item FR in the blind condition.

In particular, item MD is an index of mental demand during the task, and we confirmed that the mental workload was reduced by the haptic feedback. It should be noted that although there was no significant difference, it was suggested that the workload tended to be lower with EHF than with MHF. The item FR, an index of effort during the task, was confirmed that haptic feedback tended to decrease effort on the task compared to no haptic feedback.

4) Free Response: Regarding the difference in operability depending on the haptic conditions, 3 out of 12 participants answered that MHF was easier to operate, and 6 participants answered that EHF was better. 3 participants answered that both were about the same, or did not answer. As for MHF, some participants answered that it was highly burdensome because it was necessary to memorize the stimulus intensity and to convert the amount of movement from the intensity to the movement once in the head. In addition, the stimulus intensity decreased when the cursor position exceeded the target in EHF, and some participants answered that this change was used as a guide for manipulation.

V. Experiment 2: SuperLimbs

We investigate the effects of haptic feedback on SuperLimbs manipulation with sub-tasking in the real world.

A. Setup and Apparatus

Figure 7a shows the experimental setup. Similar to Experiment 1 (Figure 3a), participants use the same haptic and input devices and follow instructions to operate a keyboard. The key differences are that the robot arm is placed on the right side, enabling participants to use their peripheral vision to see the end-effector, and a monitor is positioned on the wall in front of them to fix their gaze.

A self-made human-scale robot arm with two degrees of freedom was used for the task as a SuperLimbs system, featuring lengths of $300\,\mathrm{mm}$ and $400\,\mathrm{mm}$ as shown in Figure 7b. It includes two servomotors (ROBOTIS DYNAMIXEL XM540-W270-R) for the root joint in parallel drive and a servomotor (Kondo Kagaku B3M-SC-1170-A) for the elbow. The end-effector with a built-in distance sensor (Pololu VL53L1X) is attached to its end. The dimensions are $175\times90\times130\mathrm{mm}$ (W$\times$H$\times$D). A servo motor (TowerPro SG90) drives the gripper's open/close mechanism. Integrated in Unity, the system controls the end-effector's maximum

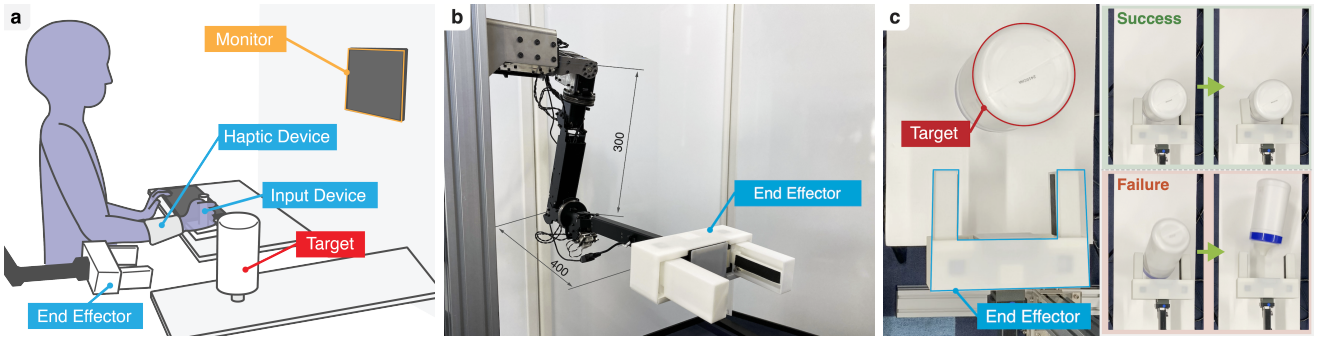

Fig. 7. (a) in the setup, the robot arm is located on the right side of a participant in the experiment, (b) robot arm with an end-effector, (c) the end-effector reaches the target and the success is determined if the target is not knocked down.

speed to be $0.5\,\mathrm{m/s}$ or less. The arm is mounted on a stand to prevent participant movement influence.

B. Task

We use a simple reaching task with a sub-task such that participants manipulate the robot arm while calculating single-digit addition. The end-effector of the robot is manipulated according to the one-dimensional axis direction, as in Experiment 1. During the manipulation, the participants' gaze is fixed at the front, but they can see the robot's movements in the peripheral vision. They manipulate the end-effector to bring it close to the target ($100\,\mathrm{mm}$ in diameter) and grasp it (Figure 7c).

The task sequence consists of three steps as below. 1) The robot moves to the initial position and an experimenter puts the target object. The initial position of the target is randomly selected from four positions (distance between the tip of the end-effector and the center of the target: 150, 200, 250, and 300mm). 2) After it's ready to operate, the participant manipulates the robot while voicing the answer to the addition. The displayed digits on the monitor are updated every second. Participants are required to move the robot as quickly and accurately as possible to the target while constantly performing the addition. 3) The participant presses a key on the keyboard with the left hand when the participant judges the end-effector has reached the target position. When the key is pressed, the end-effector closes. Success is indicated when the target is grasped, and failure is indicated when the target is knocked down or stopped in front of the arm as shown in Figure 7c. This sequence is performed for the number of times specified trials.

C. Procedure and Participants

The reaching task involves three sessions based on haptic feedback conditions (NO, MHF, EHF), without separating visual conditions as only slight differences were observed between visual conditions in Experiment 1. As with Experiment 1, Session 1 presents NO condition, while Sessions 2 and 3 present MHF or EHF, counterbalanced across participants. Sessions include practice (8 trials) without arithmetic and main trials (20 trials). For haptic feedback, positions p, p_i, and p_f correspond to the end-effector's current, initial, and the target's position. The error amount for EHF used distance sensor measurements on the end-effector. For subjective evaluation, participants complete the subjective workload questionnaire after each session and provide oral comments or feedback about the task as with Experiment 1.

The participants were each 12 healthy adults (aged between 22 and 41 with an average age of 27.4, 10 males and 2 females). All are right-handed, and four participants took part in Experiment 1.

D. Results

1) Completion Time: Figure 8 presents the results of the task completion time. The mean completion time for all conditions was $4.6\,\mathrm{s}$ (SD: $\pm 1.8\,\mathrm{s}$), and the mean completion time was 5.0, 4.6, and 4.3s, respectively, from left to right (NO, MHF, and EHF). We conducted a statistical analysis to confirm the differences because the task completion time tended to decrease in the order of NO, MHF, and EHF. Since the Shapiro-Wilk test rejected normality, we conducted the Friedman test, and it was confirmed that there was a significantly different condition ($\chi^2(2) = 25.833$, $p < 0.001$). As a post hoc test, multiple comparisons were conducted using the Wilcoxon rank sum test using Bonferroni correction, and significant differences were confirmed between NO–EHF (adj. $p < 0.001$) and MHF–EHF (adj. $p = 0.002$). These results indicate that the EHF condition significantly decreased the completion time more than the no haptic condition and that the completion time was also affected by the type of haptic feedback.

2) Success Rate and Accuracy: The results of the success rate and the task accuracy are shown in Figure 9 and Figure 10, respectively. The mean success rate was 43.3, 59.2, and 62.5%, respectively, from left to right in Figure 9, and it tends to increase in the order of NO, MHF, and EHF, in contrast to the results of the completion time. Since the Shapiro-Wilk test did not reject normality, one-way ANOVA was performed, and it was confirmed that there were significantly different conditions ($F(2, 33) = 5.512$, $p = 0.009$). As a post hoc test, multiple comparisons were conducted using the Wilcoxon rank sum test using Bonferroni correction, and significant differences were confirmed between NO–MHF (adj. $p = 0.048$) and NO–EHF (adj. $p = 0.014$).

Accuracy here refers to the distance error between the end-effector and the target when the target was successfully

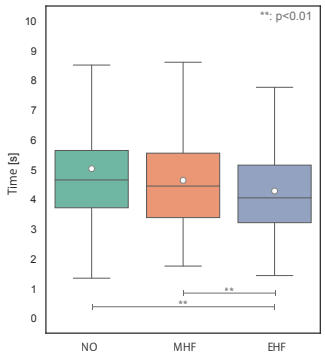

Fig. 8. Completion time

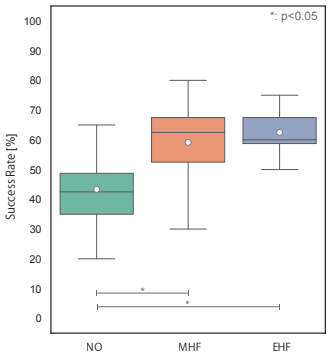

Fig. 9. Success rate

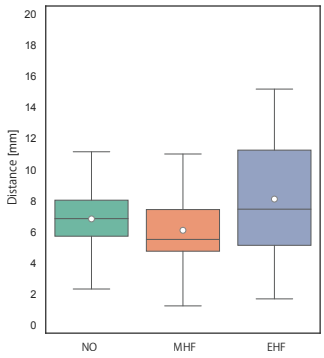

Fig. 10. Task accuracy

grasped during the trial. The mean distance error was 6.8, 6.0, and 8.7mm, respectively, from left to right in Figure 10. Since the Shapiro-Wilk test did not reject normality, one-way ANOVA was performed, and there was no significant difference ($F(2, 33) = 1.016$, $p = 0.373$). Note that comparing the distance of MHF with that of EHF, there was a tendency for EHF to have a larger variance in the distance. Although no significant difference was confirmed, this suggests that the task accuracy tends to differ depending on the haptic feedback condition.

3) Subjective Workload: Figure 11 presents the response scores of the subjective workload. The scores are converted from a 7-point Likert scale to percentages. The overall tendency of the scores is that the load of the NO condition is high, and the scores for MHF and EHF are equally low or the scores for EHF are the lowest, as in Experiment 1.

As for the statistical analysis, since the Shapiro-Wilk test rejected normality, we conducted the Friedman test. The results confirm that there was the possibility of a significant difference in the items MD ($\chi^2(2) = 9.905$, $p = 0.007$), TD ($\chi^2(2) = 6.790$, $p = 0.034$), EF ($\chi^2(2) = 10.757$, $p = 0.005$), and FR ($\chi^2(2) = 9.771$, $p = 0.008$). As a post hoc test, multiple comparisons were conducted using the Wilcoxon rank sum test using Bonferroni correction, and significant differences were found in NO–EHF for item MD (adj. $p = 0.022$), NO–EHF for item EF (adj. $p = 0.030$), and NO–EHF for item FR (adj. $p = 0.033$).

4) Free Response: In free responses, all 12 participants reported either inability to see or could see it but could not recognize its movement during the task. Some participants answered that they could only see the moment when the target fell down. One participant mentioned visibility of movement depends on the target's position. Despite not using white noise headphones to block sounds from the haptic device and robot, 11 participants didn't use sound as a cue or didn't notice it, while one reported sometimes using it. Subjective responses regarding attention allocation to sub-tasks varied, with some focusing more on the manipulation task and others on the computational task.

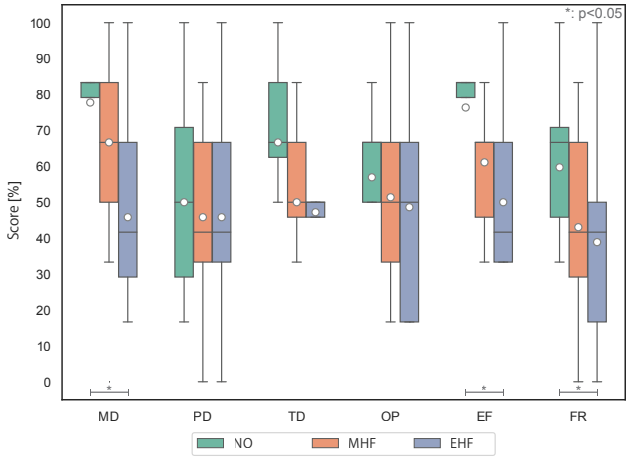

Fig. 11. Subjective task load

VI. Discussion

First, we examined how visual information influenced task performance. In Experiment 1, where visual feedback could be used, the haptic feedback condition had no significant effect in the Visual condition. However, when visual information was limited in the Blind condition, performance differed across haptic feedback conditions. A similar trend was observed when comparing Experiments 1 and 2, both of which involved restricted visual information: in the NO condition, the distance to the target was greater (Experiment 1) or the success rate was lower (Experiment 2), whereas MHF and EHF consistently improved these measures.

Next, focusing on the haptic feedback condition, we could confirm that the difference between MHF and EHF affected the results of task performance. There was no difference in the completion time between the feedback conditions in Experiment 1, but the completion time was significantly shorter in MHF and EHF than in NO in Experiment 2. Because a trial was judged as a failure when the target object was knocked over in Experiment 2, participants manipulated the object more carefully, which likely affected completion time. In EHF, participants reached the target more quickly

because the feedback conveyed distance information. The task accuracy in Experiment 2 indicates the grasp position at the time of task success. This result shows that in MHF, the user grasps the target object more closely with the end-effector, while in EHF, the user grasps the target object at a slight distance. In Experiment 1, some participants reported using changes in stimulus intensity in EHF as a cue to detect overshoot, whereas the task structure of Experiment 2 did not allow such cueing, which may partially explain the difference in task accuracy between the two experiments.

Finally, regarding subjective workload, the trend was consistent across the two experiments. Overall, NO scores were higher, and MHF and EHF scores were lower or similar in that order. In both experiments, cognitive load was significantly lower in the EHF condition compared to NO. Free responses from the interviews with the experimental participants also suggested that EHF tended to have lower cognitive load than MHF. However, the extent to which the reduced cognitive load observed in EHF and MHF will change with long-term user habituation remains unknown. Such habituation is essential for shifting from conscious estimation of haptic cues to more automatic and unconscious sensorimotor processing. Verifying this transition will be crucial for understanding how proprioception-inspired feedback can support effortless robot operation in real-world scenarios.

VII. Conclusion

In this study, we introduced a proprioception-inspired haptic feedback approach using a wearable device for robot manipulation under disturbed visual conditions. Our findings from experiments showed that haptic feedback increases task performance and reduces users' subjective workload, particularly mental demands. Further research in complex environmental conditions is expected for practical application, but we believe that the proposed approach could benefit the broader fields of HRI and HCI.

References

[1] J. Wheeler *et al.*, "Investigation of rotational skin stretch for proprioceptive feedback with application to myoelectric systems," *IEEE Trans. Neural Syst. Rehabil. Eng.*, vol. 18, no. 1, 58–66, Feb. 2010.

[2] M. Rossi *et al.*, "HapPro: A wearable haptic device for proprioceptive feedback," *IEEE Trans. Biomed. Eng.*, vol. 66, no. 1, 138–149, Jan. 2019.

[3] N. Colella *et al.*, "A novel Skin-Stretch haptic device for intuitive control of robotic prostheses and avatars," *IEEE Robotics and Automation Letters*, vol. 4, no. 2, 1572–1579, Apr. 2019.

[4] L. Meli *et al.*, "The hbracelet: A wearable haptic device for the distributed mechanotactile stimulation of the upper limb," *IEEE Robotics and Automation Letters*, vol. 3, no. 3, 2198–2205, Jul. 2018.

[5] J. Bimbo *et al.*, "Teleoperation in cluttered environments using wearable haptic feedback," in *2017 IEEE/RSJ International Conference on Intelligent Robots and Systems (IROS)*, Sep. 2017, 3401–3408.

[6] D. P. Losey *et al.*, "A review of intent detection, arbitration, and communication aspects of shared control for physical Human–Robot interaction," *Appl. Mech. Rev.*, vol. 70, no. 1, p. 010804, Feb. 2018.

[7] I. Hussain *et al.*, "Using the robotic sixth finger and vibrotactile feedback for grasp compensation in chronic stroke patients," in *2015 IEEE International Conference on Rehabilitation Robotics (ICORR)*. ieeexplore.ieee.org, Aug. 2015, 67–72.

[8] T. Sasaki *et al.*, "MetaLimbs: multiple arms interaction metamorphism," in *ACM SIGGRAPH 2017 Emerging Technologies*, ser. SIGGRAPH '17, no. Article 16. New York, NY, USA: Association for Computing Machinery, Jul. 2017, 1–2.

[9] E. P. Gardner and J. H. Martin, "Coding of sensory information," *Principles of neural science*, 2000.

[10] C. Ghez, J. Gordon, and M. F. Ghilardi, "Impairments of reaching movements in patients without proprioception. II. effects of visual information on accuracy," *J. Neurophysiol.*, vol. 73, no. 1, 361–372, Jan. 1995.

[11] C. Pacchierotti *et al.*, "Wearable haptic systems for the fingertip and the hand: Taxonomy, review, and perspectives," *IEEE Trans. Haptics*, vol. 10, no. 4, 580–600, Oct. 2017.

[12] H. Culbertson, S. B. Schorr, and A. M. Okamura, "Haptics: The present and future of artificial touch sensation," *Annu. Rev. Control Robot. Auton. Syst.*, vol. 1, no. 1, 385–409, May 2018.

[13] P. B. Shull and D. D. Damian, "Haptic wearables as sensory replacement, sensory augmentation and trainer - a review," *J. Neuroeng. Rehabil.*, vol. 12, p. 59, Jul. 2015.

[14] Z. A. Zook *et al.*, "Effect of interference on Multi-Sensory haptic perception of stretch and squeeze," 2019.

[15] K. Minamizawa and S. Fukamachi, "Gravity grabber: wearable haptic display to present virtual mass sensation," *ACM SIGGRAPH 2007 emerging technologies*, p. 8, 2007.

[16] S. Casini *et al.*, "Design and realization of the CUFF - clenching upper-limb force feedback wearable device for distributed mechano-tactile stimulation of normal and tangential skin forces," in *2015 IEEE/RSJ International Conference on Intelligent Robots and Systems (IROS)*, Sep. 2015, 1186–1193.

[17] I. Han and J. Park, "Continuous Skin-Stretch feedback for rendering 3D vector information," *IEEE Access*, vol. 8, 145 649–145 660, 2020.

[18] K. Bark *et al.*, "Comparison of skin stretch and vibrotactile stimulation for feedback of proprioceptive information," in *2008 Symposium on Haptic Interfaces for Virtual Environment and Teleoperator Systems*, Mar. 2008, 71–78.

[19] M. Aggravi *et al.*, "Design and evaluation of a wearable haptic device for skin stretch, pressure, and vibrotactile stimuli," *IEEE Robotics and Automation Letters*, vol. 3, no. 3, 2166–2173, Jul. 2018.

[20] E. Pezent *et al.*, "Tasbi: Multisensory squeeze and vibrotactile wrist haptics for augmented and virtual reality," in *2019 IEEE World Haptics Conference (WHC)*, Jul. 2019, 1–6.

[21] S. Choi and K. J. Kuchenbecker, "Vibrotactile display: Perception, technology, and applications," *Proc. IEEE*, vol. 101, no. 9, 2093–2104, Sep. 2013.

[22] N. Dunkelberger *et al.*, "Conveying language through haptics: a multi-sensory approach," in *Proceedings of the 2018 ACM International Symposium on Wearable Computers*, ser. ISWC '18. New York, NY, USA: Association for Computing Machinery, Oct. 2018, 25–32.

[23] M. Selvaggio *et al.*, "Autonomy in physical human-robot interaction: A brief survey," *IEEE Robotics and Automation Letters*, vol. 6, no. 4, 7989–7996, Oct. 2021.

[24] L. Mart *et al.*, "Development of a combination device of vibration tactile device and tightening device to realize human-robot handover operation," *IEEE Robot. Autom. Lett.*, vol. 10, no. 4, 4109–4116, Apr. 2025.

[25] B. Llorens-Bonilla, F. Parietti, and H. H. Asada, "Demonstration-based control of supernumerary robotic limbs," *Intelligent Robots and Systems (IROS), 2012 IEEE/RSJ International Conference on*, no. Figure 1, 3936–3942, 2012.

[26] Y. Tong and J. Liu, "Review of research and development of supernumerary robotic limbs," *IEEE/CAA Journal of Automatica Sinica*, vol. 8, no. 5, 929–952, May 2021.

[27] D. Prattichizzo *et al.*, "Human augmentation by wearable supernumerary robotic limbs: review and perspectives," *Prog. Biomed. Eng.*, vol. 3, no. 4, p. 042005, Sep. 2021.

[28] M. H. D. Yamen Saraiji *et al.*, "MetaArms: Body remapping using Feet-Controlled artificial arms," *The 31st Annual ACM Symposium on User Interface Software and Technology - UIST '18*, 65–74, 2018.

[29] J. W. Guggenheim and H. H. Asada, "Inherent haptic feedback from supernumerary robotic limbs," *IEEE Trans. Haptics*, vol. 4, no. 3, 1–9, 2020.

[30] Y. Iwasaki *et al.*, "Detachable body: The impact of binocular disparity and vibrotactile feedback in Co-Presence tasks," *IEEE Robotics and Automation Letters*, vol. 5, no. 2, 3477–3484, Apr. 2020.

[31] S. G. Hart and L. E. Staveland, "Development of NASA-TLX (task load index): Results of empirical and theoretical research," in *Advances in Psychology*, P. A. Hancock and N. Meshkati, Eds. North-Holland, Jan. 1988, vol. 52, 139–183.